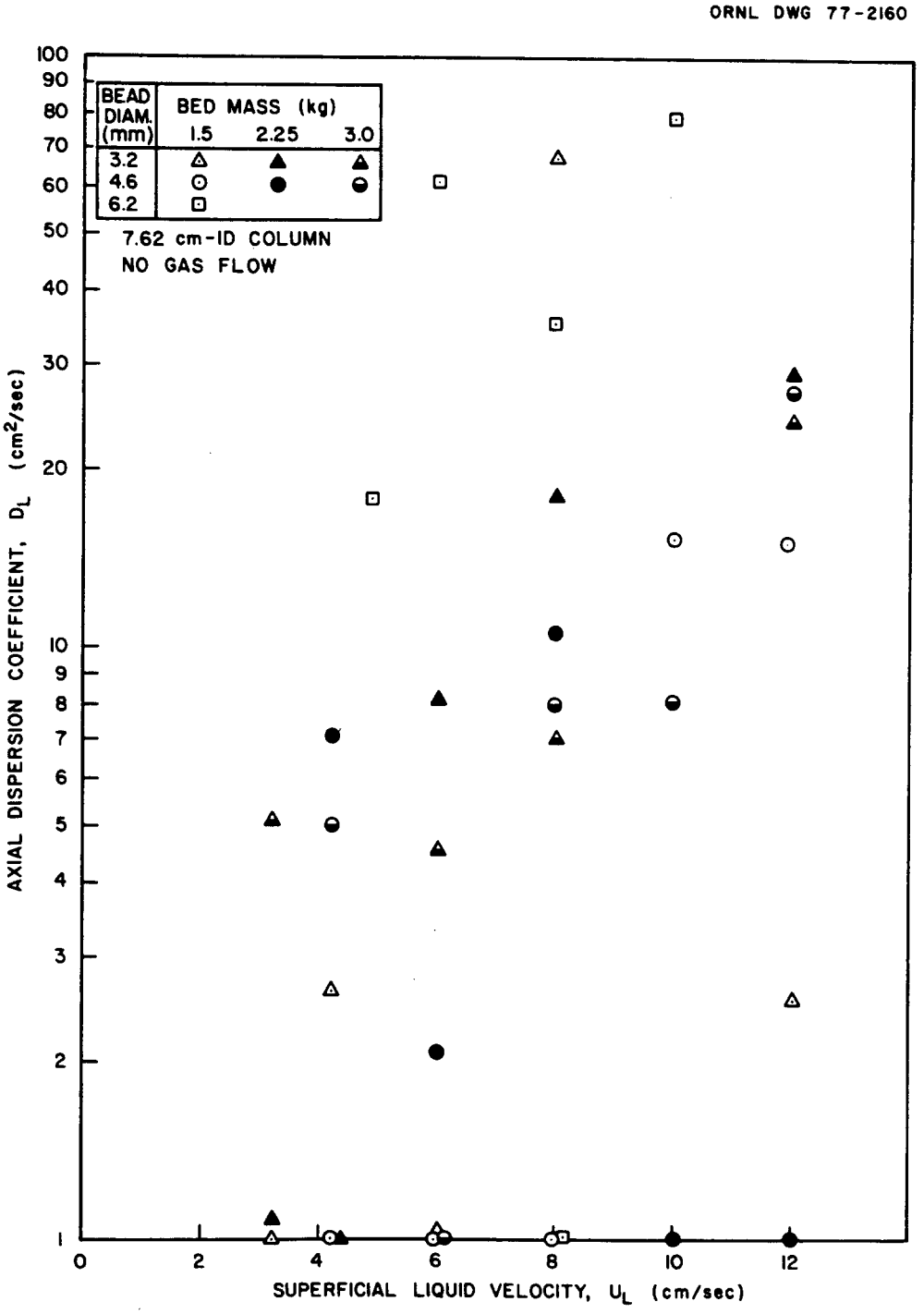

Fig. 2.26. Effect of bed mass loading on the liquid-phase axial dispersion coefficient.

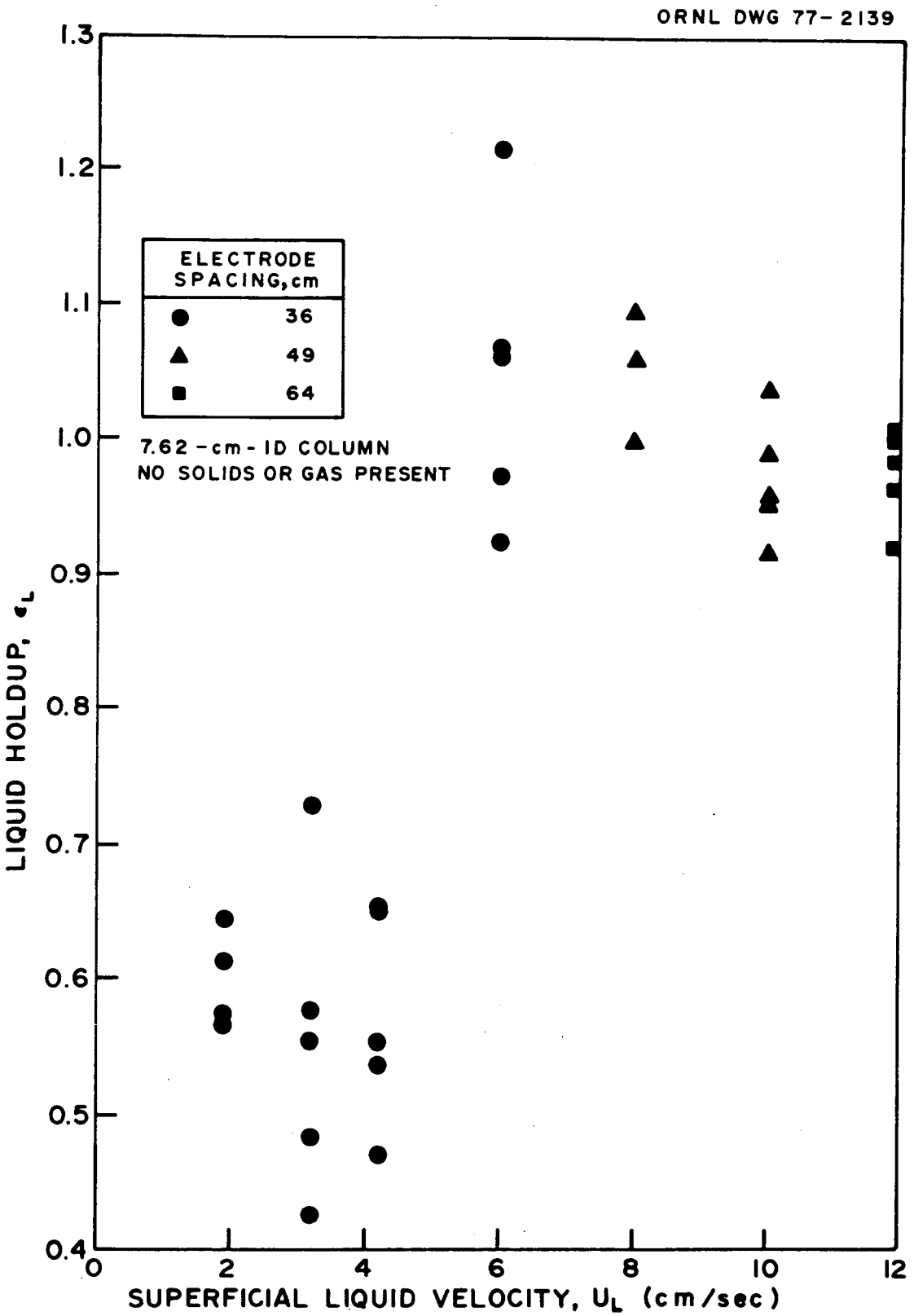

Fig. 2.27. Liquid holdups in a single-phase column calculated from the RTD curves.

and (2) equipment response times that are too long in comparison to the residence time of the tracer between each set of electrodes. In some cases, the second set of electrodes actually responded to a pulse of tracer before the first set of electrodes. This effect, which occurred mainly in highly turbulent beds in which the electrodes were closely spaced, could be reduced by separating the two sets of electrodes axially in the columns or by redesigning the electrodes so that the individual plates would be closer together. The cocurrent flow of the tracer with the liquid and gas phases resulted in very short residence times. However, precision was also limited by the fast response time required of the equipment. For example, at a superficial liquid velocity of 5 cm/sec, the liquid holdup would be typically less than 0.5, giving a real liquid velocity greater than 10 cm/sec. Thus, for an electrode spacing of 30 cm, the residence time would be less than 3 sec. Worse yet, the tracer pulse would pass through each set of electrodes (1 cm x 1 cm in size) in less than 0.1 sec. The problem of residence time through the electrode itself will require more sophisticated equipment than is currently available.

Mass transfer. The liquid-phase mass transfer data were analyzed using both the PF and CSTR models as described previously.[36] Tables 2.12-2.15 present the results for the three sizes of glass beads and the single size of plexiglass beads.

The effect of gas velocity on the overall volumetric mass transfer coefficient, $K_L a$, for beds of 6.3-mm-diam plexiglass beads is shown in Fig. 2.28. The mass transfer coefficient increased with both increasing liquid and gas velocities. This result is qualitatively typical of those found for each of the solids studied (Figs. 2.29-2.31). However, as these

Table 2.12. Mass transfer data for beds of 4.6-mm-diam glass beads

RUN NUMBER	GAS VEL. (CM/S)	LIQUID VEL. (CM/S)	PORT HEIGHT (CM)	NTU[a] PF	NTU[a] CSTR	KLA PF (1/S)	KLA CSTR (1/S)
G04APV3	4.47	2.98	33.0	0.639	0.893	0.058	0.081
G05APX3	5.17	6.20	49.0	0.224	0.251	0.028	0.032
G06APX3	4.83	6.20	33.0	0.007	0.007	0.001	0.001
G06APX3	4.83	6.20	49.0	0.311	0.365	0.039	0.046
G07APW3	4.53	5.25	49.0	0.295	0.343	0.032	0.037
G08APW3	4.48	5.25	49.0	0.874	1.388	0.094	0.149
G08APW3	4.48	5.25	33.0	0.759	1.131	0.121	0.180
G08APW3	4.48	5.25	17.0	0.388	0.474	0.120	0.146
G09APW3	4.49	5.25	49.0	0.695	1.000	0.074	0.107
G09APW3	4.49	5.25	33.0	0.681	0.972	0.108	0.155
G09APW3	4.49	5.25	17.0	0.447	0.563	0.138	0.174
G10APX3	4.50	6.20	49.0	0.676	0.962	0.086	0.122
G10APX3	4.50	6.20	33.0	0.669	0.949	0.126	0.178
G10APX3	4.50	6.20	17.0	0.427	0.531	0.156	0.194
G11APY3	4.49	8.35	49.0	0.634	0.880	0.108	0.150
G11APY3	4.49	8.35	33.0	0.624	0.861	0.158	0.218
G11APY3	4.49	8.35	17.0	0.371	0.449	0.182	0.220
G12APV3	4.47	10.27	49.0	0.662	0.933	0.139	0.196
G12APV3	4.47	10.27	33.0	0.601	0.818	0.187	0.255
G12APV3	4.47	10.27	17.0	0.366	0.441	0.221	0.267
G13BPW3	8.99	5.25	49.0	0.889	1.428	0.095	0.153
G13BPW3	8.99	5.25	33.0	0.905	1.466	0.144	0.233
G13BPW3	8.99	5.25	17.0	0.795	1.210	0.245	0.374
G14BPX3	9.00	6.20	49.0	0.815	1.255	0.103	0.159
G14BPX3	9.00	6.20	33.0	0.861	1.359	0.162	0.255
G14BPX3	9.00	6.20	17.0	0.727	1.066	0.265	0.389
G15BPY3	9.00	8.35	49.0	0.733	1.078	0.125	0.184
G15BPY3	9.00	8.35	33.0	0.707	1.023	0.179	0.259
G15BPY3	9.00	8.35	17.0	0.477	0.610	0.234	0.300
G16AW3	4.99	5.25	49.0	0.675	0.961	0.072	0.103
G16AW3	4.99	5.25	33.0	0.643	0.899	0.102	0.143
G16AW3	4.99	5.25	17.0	0.277	0.319	0.086	0.099
G17AX3	4.99	6.20	49.0	0.687	0.984	0.087	0.125
G17AX3	4.99	6.20	33.0	0.673	0.957	0.127	0.180
G17AX3	4.99	6.20	17.0	0.357	0.429	0.130	0.157
G18AY3	4.99	8.35	49.0	0.632	0.878	0.108	0.150
G18AY3	4.99	8.35	33.0	0.609	0.835	0.154	0.211
G18AY3	4.99	8.35	17.0	0.203	0.225	0.100	0.110
G19AZ3	4.99	12.33	49.0	0.718	1.040	0.181	0.262
G19AZ3	4.99	12.33	33.0	0.701	1.006	0.262	0.376
G19AZ3	4.99	12.33	17.0	0.243	0.274	0.176	0.199
G20BW3	9.86	5.25	49.0	0.890	1.430	0.095	0.153
G20BW3	9.86	5.25	33.0	0.964	1.614	0.153	0.257
G20BW3	9.86	5.25	17.0	0.902	1.459	0.278	0.451
G21BX3	9.85	6.20	49.0	0.889	1.428	0.113	0.181
G21BX3	9.85	6.20	33.0	0.882	1.410	0.166	0.265
G21BX3	9.85	6.20	17.0	0.806	1.235	0.294	0.451
G22BY3	9.85	8.35	49.0	0.776	1.168	0.132	0.199
G22BY3	9.85	8.35	33.0	0.729	1.070	0.185	0.271
G22BY3	9.85	8.35	17.0	0.597	0.815	0.293	0.400
G23BZ3	9.71	12.33	49.0	0.804	1.227	0.202	0.309
G23BZ3	9.71	12.33	33.0	0.717	1.044	0.268	0.390
G23BZ3	9.71	12.33	17.0	0.539	0.712	0.390	0.516
G24CW3	14.79	5.25	49.0	1.085	1.952	0.116	0.209
G24CW3	14.79	5.25	33.0	1.156	2.167	0.184	0.345
G24CW3	14.79	5.25	17.0	0.956	1.598	0.295	0.493
G25CX3	14.80	6.20	49.0	1.017	1.759	0.129	0.223
G25CX3	14.80	6.20	33.0	1.006	1.727	0.189	0.325
G25CX3	14.80	6.20	17.0	0.734	1.081	0.268	0.394
G26CY3	14.79	8.35	49.0	0.850	1.335	0.145	0.228
G26CY3	14.79	8.35	33.0	0.834	1.298	0.211	0.328
G26CY3	14.79	8.35	17.0	0.652	0.918	0.320	0.451
G27CY3	14.78	10.27	49.0	0.838	1.306	0.176	0.274
G27CY3	14.78	10.27	33.0	0.793	1.206	0.247	0.375
G27CY3	14.78	10.27	17.0	0.582	0.789	0.352	0.476
G28CZ3	14.63	12.33	49.0	0.827	1.280	0.208	0.322
G28CZ3	14.63	12.33	33.0	0.786	1.190	0.294	0.445
G28CZ3	14.63	12.33	17.0	0.570	0.767	0.413	0.556

Table 2.12 (Cont'd)

RUN NUMBER	GAS VEL. (CM/S)	LIQUID VEL. (CM/S)	PORT HEIGHT (CM)	NTU[a] PF	NTU[a] CSTR	KLA PF (1/S)	KLA CSTR (1/S)
G04APV3	4.47	2.98	33.0	0.639	0.893	0.058	0.081
G05APX3	5.17	6.20	49.0	0.224	0.251	0.028	0.032
G06APX3	4.83	6.20	33.0	0.007	0.007	0.001	0.001
G06APX3	4.83	6.20	49.0	0.311	0.365	0.039	0.046
G07APW3	4.53	5.25	49.0	0.295	0.343	0.032	0.037
G08APW3	4.48	5.25	49.0	0.874	1.388	0.094	0.149
G08APW3	4.48	5.25	33.0	0.759	1.131	0.121	0.180
G08APW3	4.48	5.25	17.0	0.388	0.474	0.120	0.146
G09APW3	4.49	5.25	49.0	0.695	1.000	0.074	0.107
G09APW3	4.49	5.25	33.0	0.681	0.972	0.108	0.155
G09APW3	4.49	5.25	17.0	0.447	0.563	0.138	0.174
G10APX3	4.50	6.20	49.0	0.676	0.962	0.086	0.122
G10APX3	4.50	6.20	33.0	0.669	0.949	0.126	0.178
G10APX3	4.50	6.20	17.0	0.427	0.531	0.156	0.194
G11APY3	4.49	8.35	49.0	0.634	0.880	0.108	0.150
G11APY3	4.49	8.35	33.0	0.624	0.861	0.158	0.218
G11APY3	4.49	8.35	17.0	0.371	0.449	0.182	0.220
G12APV3	4.47	10.27	49.0	0.662	0.933	0.139	0.196
G12APV3	4.47	10.27	33.0	0.601	0.818	0.187	0.255
G12APV3	4.47	10.27	17.0	0.366	0.441	0.221	0.267
G13BPW3	8.99	5.25	49.0	0.889	1.428	0.095	0.153
G13BPW3	8.99	5.25	33.0	0.905	1.466	0.144	0.233
G13BPW3	8.99	5.25	17.0	0.795	1.210	0.245	0.374
G14BPX3	9.00	6.20	49.0	0.815	1.255	0.103	0.159
G14BPX3	9.00	6.20	33.0	0.861	1.359	0.162	0.255
G14BPX3	9.00	6.20	17.0	0.727	1.066	0.265	0.389
G15BPY3	9.00	8.35	49.0	0.733	1.078	0.125	0.184
G15BPY3	9.00	8.35	33.0	0.707	1.023	0.179	0.259
G15BPY3	9.00	8.35	17.0	0.477	0.610	0.234	0.300
G16AW3	4.99	5.25	49.0	0.675	0.961	0.072	0.103
G16AW3	4.99	5.25	33.0	0.643	0.899	0.102	0.143
G16AW3	4.99	5.25	17.0	0.277	0.319	0.086	0.099
G17AX3	4.99	6.20	49.0	0.687	0.984	0.087	0.125
G17AX3	4.99	6.20	33.0	0.673	0.957	0.127	0.180
G17AX3	4.99	6.20	17.0	0.357	0.429	0.130	0.157
G18AY3	4.99	8.35	49.0	0.632	0.878	0.108	0.150
G18AY3	4.99	8.35	33.0	0.609	0.835	0.154	0.211
G18AY3	4.99	8.35	17.0	0.203	0.225	0.100	0.110
G19AZ3	4.99	12.33	49.0	0.718	1.040	0.181	0.262
G19AZ3	4.99	12.33	33.0	0.701	1.006	0.262	0.376
G19AZ3	4.99	12.33	17.0	0.243	0.274	0.176	0.199
G20BW3	9.86	5.25	49.0	0.890	1.430	0.095	0.153
G20BW3	9.86	5.25	33.0	0.964	1.614	0.153	0.257
G20BW3	9.86	5.25	17.0	0.902	1.459	0.278	0.451
G21BX3	9.85	6.20	49.0	0.889	1.428	0.113	0.181
G21BX3	9.85	6.20	33.0	0.882	1.410	0.166	0.265
G21BX3	9.85	6.20	17.0	0.806	1.235	0.294	0.451
G22BY3	9.85	8.35	49.0	0.776	1.168	0.132	0.199
G22BY3	9.85	8.35	33.0	0.729	1.070	0.185	0.271
G22BY3	9.85	8.35	17.0	0.597	0.815	0.293	0.400
G23BZ3	9.71	12.33	49.0	0.804	1.227	0.202	0.309
G23BZ3	9.71	12.33	33.0	0.717	1.044	0.268	0.390
G23BZ3	9.71	12.33	17.0	0.539	0.712	0.390	0.516
G24CW3	14.79	5.25	49.0	1.085	1.952	0.116	0.209
G24CW3	14.79	5.25	33.0	1.156	2.167	0.184	0.345
G24CW3	14.79	5.25	17.0	0.956	1.598	0.295	0.493
G25CX3	14.80	6.20	49.0	1.017	1.759	0.129	0.223
G25CX3	14.80	6.20	33.0	1.006	1.727	0.189	0.325
G25CX3	14.80	6.20	17.0	0.734	1.081	0.268	0.394
G26CY3	14.79	8.35	49.0	0.850	1.335	0.145	0.228
G26CY3	14.79	8.35	33.0	0.834	1.298	0.211	0.328
G26CY3	14.79	8.35	17.0	0.652	0.918	0.320	0.451
G27CY3	14.78	10.27	49.0	0.838	1.306	0.176	0.274
G27CY3	14.78	10.27	33.0	0.793	1.206	0.247	0.375
G27CY3	14.78	10.27	17.0	0.582	0.789	0.352	0.476
G28CZ3	14.63	12.33	49.0	0.827	1.280	0.208	0.322
G28CZ3	14.63	12.33	33.0	0.786	1.190	0.294	0.445
G28CZ3	14.63	12.33	17.0	0.570	0.767	0.413	0.556

[a]NTU = number of transfer units.

Table 2.13. Mass transfer data for beds of 3.2-mm-diam glass beads

RUN NUMBER	GAS VEL. (CM/S)	LIQUID VEL. (CM/S)	PORT HEIGHT (CM)	NTU[a] PF	NTU[a] CSTR	KLA PF (1/S)	KLA CSTR (1/S)
C01AXP3	5.02	5.25	49.0	0.351	0.420	0.038	0.045
C01AXP3	5.02	5.25	33.0	0.296	0.344	0.047	0.055
C01AXP3	5.02	5.25	17.0	0.183	0.201	0.056	0.062
C02AY3	5.02	6.20	49.0	0.316	0.371	0.040	0.047
C02AY3	5.02	6.20	33.0	0.280	0.323	0.053	0.061
C02AY3	5.02	6.20	17.0	0.216	0.241	0.079	0.088
C03AZ3	5.02	8.35	49.0	0.283	0.327	0.048	0.056
C03AZ3	5.02	8.35	33.0	0.275	0.317	0.070	0.080
C03AZ3	5.02	8.35	17.0	0.219	0.244	0.107	0.120
C04AZP3	4.95	12.33	49.0	0.409	0.503	0.103	0.127
C04AZP3	4.95	12.33	33.0	0.405	0.498	0.151	0.186
C04AZP3	4.95	12.33	17.0	0.354	0.424	0.257	0.307
C05BXP3	9.85	5.25	49.0	0.560	0.750	0.060	0.080
C05BXP3	9.85	5.25	33.0	0.556	0.742	0.088	0.118
C05BXP3	9.85	5.25	17.0	0.458	0.581	0.142	0.179
C06BY3	9.87	6.20	49.0	0.542	0.718	0.069	0.091
C06BY3	9.87	6.20	33.0	0.467	0.595	0.088	0.112
C06BY3	9.87	6.20	17.0	0.372	0.450	0.136	0.164
C07BZ3	9.85	8.35	49.0	0.473	0.604	0.081	0.103
C07BZ3	9.85	8.35	33.0	0.381	0.463	0.096	0.117
C07BZ3	9.85	8.35	17.0	0.309	0.362	0.152	0.178
C08BZP3	9.74	12.33	49.0	0.572	0.770	0.144	0.194
C08BZP3	9.74	12.33	33.0	0.485	0.623	0.181	0.233
C08BZP3	9.74	12.33	17.0	0.398	0.488	0.288	0.354
C09CXP3	14.83	5.25	49.0	0.711	1.035	0.076	0.111
C09CXP3	14.83	5.25	33.0	0.667	0.947	0.106	0.151
C09CXP3	14.83	5.25	17.0	0.596	0.814	0.184	0.251
C10CY3	14.90	6.20	49.0	0.661	0.936	0.084	0.118
C10CY3	14.90	6.20	33.0	0.551	0.734	0.104	0.138
C10CY3	14.90	6.20	17.0	0.488	0.628	0.178	0.229
C11CZ3	14.90	8.35	49.0	0.574	0.774	0.098	0.132
C11CZ3	14.90	8.35	33.0	0.463	0.588	0.117	0.149
C11CZ3	14.90	8.35	17.0	0.384	0.468	0.189	0.230
C12CW3	14.86	3.58	49.0	0.935	1.544	0.068	0.113
C12CW3	14.86	3.58	33.0	1.013	1.750	0.110	0.190
C12CW3	14.86	3.58	17.0	1.080	1.939	0.227	0.408
C13CX3	14.86	4.29	49.0	0.836	1.305	0.073	0.114
C13CX3	14.86	4.29	33.0	0.813	1.252	0.106	0.163
C13CX3	14.86	4.29	17.0	0.880	1.409	0.222	0.356
C14AW3	5.05	3.58	49.0	0.438	0.549	0.032	0.040
C14AW3	5.05	3.58	33.0	0.392	0.479	0.042	0.052
C14AW3	5.05	3.58	17.0	0.195	0.215	0.041	0.045
C15AX3	5.05	4.29	49.0	0.387	0.471	0.034	0.041
C15AX3	5.05	4.29	33.0	0.426	0.531	0.055	0.069
C15AX3	5.05	4.29	17.0	0.252	0.286	0.064	0.072
C16BX3	9.92	4.29	49.0	0.606	0.833	0.053	0.073
C16BX3	9.92	4.29	33.0	0.692	0.995	0.090	0.130
C16BX3	9.92	4.29	17.0	0.702	1.016	0.177	0.257
C17BW3	9.92	3.58	49.0	0.712	1.037	0.052	0.076
C17BW3	9.92	3.58	33.0	0.830	1.292	0.090	0.140
C17BW3	9.92	3.58	17.0	0.604	0.830	0.127	0.175

Table 2.13. (Cont'd)

RUN NUMBER	GAS VEL. (CM/S)	LIQUID VEL. (CM/S)	PORT HEIGHT (CM)	NTU[a] PF	NTU[a] CSTR	KLA PF (1/S)	KLA CSTR (1/S)
C01AXP3	5.02	5.25	49.0	0.351	0.420	0.038	0.045
C01AXP3	5.02	5.25	33.0	0.296	0.344	0.047	0.055
C01AXP3	5.02	5.25	17.0	0.183	0.201	0.056	0.062
C02AY3	5.02	6.20	49.0	0.316	0.371	0.040	0.047
C02AY3	5.02	6.20	33.0	0.280	0.323	0.053	0.061
C02AY3	5.02	6.20	17.0	0.216	0.241	0.079	0.088
C03AZ3	5.02	8.35	49.0	0.283	0.327	0.048	0.056
C03AZ3	5.02	8.35	33.0	0.275	0.317	0.070	0.080
C03AZ3	5.02	8.35	17.0	0.219	0.244	0.107	0.120
C04AZP3	4.95	12.33	49.0	0.409	0.503	0.103	0.127
C04AZP3	4.95	12.33	33.0	0.405	0.498	0.151	0.186
C04AZP3	4.95	12.33	17.0	0.354	0.424	0.257	0.307
C05BXP3	9.85	5.25	49.0	0.560	0.750	0.060	0.080
C05BXP3	9.85	5.25	33.0	0.556	0.742	0.088	0.118
C05BXP3	9.85	5.25	17.0	0.458	0.581	0.142	0.179
C06BY3	9.87	6.20	49.0	0.542	0.718	0.069	0.091
C06BY3	9.87	6.20	33.0	0.467	0.595	0.088	0.112
C06BY3	9.87	6.20	17.0	0.372	0.450	0.136	0.164
C07BZ3	9.85	8.35	49.0	0.473	0.604	0.081	0.103
C07BZ3	9.85	8.35	33.0	0.381	0.463	0.096	0.117
C07BZ3	9.85	8.35	17.0	0.309	0.362	0.152	0.178
C08BZP3	9.74	12.33	49.0	0.572	0.770	0.144	0.194
C08BZP3	9.74	12.33	33.0	0.485	0.623	0.181	0.233
C08BZP3	9.74	12.33	17.0	0.398	0.488	0.288	0.354
C09CXP3	14.83	5.25	49.0	0.711	1.035	0.076	0.111
C09CXP3	14.83	5.25	33.0	0.667	0.947	0.106	0.151
C09CXP3	14.83	5.25	17.0	0.596	0.814	0.184	0.251
C10CY3	14.90	6.20	49.0	0.661	0.936	0.084	0.118
C10CY3	14.90	6.20	33.0	0.551	0.734	0.104	0.138
C10CY3	14.90	6.20	17.0	0.488	0.628	0.178	0.229
C11CZ3	14.90	8.35	49.0	0.574	0.774	0.098	0.132
C11CZ3	14.90	8.35	33.0	0.463	0.588	0.117	0.149
C11CZ3	14.90	8.35	17.0	0.384	0.468	0.189	0.230
C12CW3	14.86	3.58	49.0	0.935	1.544	0.068	0.113
C12CW3	14.86	3.58	33.0	1.013	1.750	0.110	0.190
C12CW3	14.86	3.58	17.0	1.080	1.939	0.227	0.408
C13CX3	14.86	4.29	49.0	0.836	1.305	0.073	0.114
C13CX3	14.86	4.29	33.0	0.813	1.252	0.106	0.163
C13CX3	14.86	4.29	17.0	0.880	1.409	0.222	0.356
C14AW3	5.05	3.58	49.0	0.438	0.549	0.032	0.040
C14AW3	5.05	3.58	33.0	0.392	0.479	0.042	0.052
C14AW3	5.05	3.58	17.0	0.195	0.215	0.041	0.045
C15AX3	5.05	4.29	49.0	0.387	0.471	0.034	0.041
C15AX3	5.05	4.29	33.0	0.426	0.531	0.055	0.069
C15AX3	5.05	4.29	17.0	0.252	0.286	0.064	0.072
C16BX3	9.92	4.29	49.0	0.606	0.833	0.053	0.073
C16BX3	9.92	4.29	33.0	0.692	0.995	0.090	0.130
C16BX3	9.92	4.29	17.0	0.702	1.016	0.177	0.257
C17BW3	9.92	3.58	49.0	0.712	1.037	0.052	0.076
C17BW3	9.92	3.58	33.0	0.830	1.292	0.090	0.140
C17BW3	9.92	3.58	17.0	0.604	0.830	0.127	0.175

[a] NTU = number of transfer units.

Table 2.14. Mass transfer data for beds of 6.2-mm-diam glass beads

RUN NUMBER	GAS VEL. (CM/S)	LIQUID VEL. (CM/S)	PORT HEIGHT (CM)	NTU[a] PF	NTU[a] CSTR	KLA PF (1/S)	KLA CSTR (1/S)
K01AW3	5.02	6.20	49.0	0.765	1.143	0.097	0.145
K01AW3	5.02	6.20	33.0	0.707	1.022	0.133	0.192
K01AW3	5.02	6.20	17.0	0.266	0.305	0.097	0.111
K02AX3	5.02	7.40	49.0	0.733	1.074	0.111	0.162
K02AX3	5.02	7.40	33.0	0.664	0.937	0.149	0.210
K02AX3	5.02	7.40	17.0	0.301	0.351	0.131	0.153
K03AY3	5.02	9.98	49.0	0.691	0.989	0.141	0.201
K03AY3	5.02	9.98	33.0	0.516	0.673	0.156	0.203
K03AY3	5.02	9.98	17.0	0.269	0.308	0.158	0.181
K04AZ3	5.00	14.97	49.0	0.670	0.945	0.205	0.289
K04AZ3	5.00	14.97	33.0	0.545	0.721	0.247	0.327
K04AZ3	5.00	14.97	17.0	0.382	0.464	0.337	0.409
K05BW3	9.97	6.20	49.0	0.783	1.184	0.099	0.150
K05BW3	9.97	6.20	33.0	0.831	1.291	0.156	0.243
K05BW3	9.97	6.20	17.0	0.485	0.624	0.177	0.228
K06BX3	9.97	7.40	49.0	0.765	1.145	0.115	0.173
K06BX3	9.97	7.40	33.0	0.899	1.450	0.202	0.325
K06BX3	9.97	7.40	17.0	0.549	0.731	0.239	0.318
K07BY3	9.94	9.98	49.0	0.762	1.138	0.155	0.232
K07BY3	9.94	9.98	33.0	0.765	1.143	0.231	0.346
K07BY3	9.94	9.98	17.0	0.546	0.724	0.320	0.425
K08BZ3	9.86	14.97	49.0	0.867	1.368	0.265	0.418
K08BZ3	9.86	14.97	33.0	0.750	1.110	0.340	0.503
K08BZ3	9.86	14.97	17.0	0.503	0.652	0.443	0.574
K09CW3	15.03	6.20	49.0	0.995	1.698	0.126	0.215
K09CW3	15.03	6.20	33.0	1.445	3.209	0.272	0.603
K09CW3	15.03	6.20	17.0	0.833	1.298	0.304	0.474
K10CX3	15.03	7.40	49.0	0.947	1.572	0.143	0.237
K10CX3	15.03	7.40	33.0	0.903	1.461	0.202	0.328
K10CX3	15.03	7.40	17.0	0.738	1.089	0.321	0.474
K11CY3	14.81	9.98	49.0	0.849	1.333	0.173	0.271
K11CY3	14.81	9.98	33.0	0.778	1.174	0.235	0.355
K11CY3	14.81	9.98	17.0	0.585	0.794	0.344	0.466
K12CZ3	14.61	14.97	49.0	0.851	1.334	0.260	0.407
K12CZ3	14.61	14.97	33.0	0.767	1.148	0.348	0.520
K12CZ3	14.61	14.97	17.0	0.600	0.820	0.528	0.722

[a]NTU = number of transfer units.

Table 2.15. Mass transfer data for beds of 6.3-mm-diam plexiglass beads

RUN NUMBER	GAS VEL. (CM/S)	LIQUID VEL. (CM/S)	PORT HEIGHT (CM)	NTU[a] PF	NTU[a] CSTR	KLA PF (1/S)	KLA CSTR (1/S)
P01AW3	5.11	2.15	49.0	0.750	1.114	0.033	0.049
P01AW3	5.11	2.15	33.0	0.829	1.287	0.054	0.084
P01AW3	5.11	2.15	17.0	0.757	1.130	0.096	0.143
P02AX3	5.08	2.62	49.0	0.693	0.997	0.037	0.053
P02AX3	5.08	2.62	33.0	0.700	1.011	0.056	0.080
P02AX3	5.08	2.62	17.0	0.586	0.796	0.090	0.123
P03AY3	5.08	3.46	49.0	0.624	0.865	0.044	0.061
P03AY3	5.08	3.46	33.0	0.546	0.725	0.057	0.076
P03AY3	5.08	3.46	17.0	0.383	0.466	0.078	0.095
P04AZ3	5.08	5.25	49.0	0.482	0.619	0.052	0.066
P04AZ3	5.08	5.25	33.0	0.387	0.473	0.062	0.075
P04AZ3	5.08	5.25	17.0	0.227	0.255	0.070	0.079
P05BW3	9.96	2.15	49.0	1.177	2.236	0.052	0.098
P05BW3	9.96	2.15	33.0	1.224	2.394	0.080	0.156
P05BW3	9.96	2.15	17.0	0.926	1.522	0.117	0.192
P06BX3	9.97	2.62	49.0	1.159	2.180	0.062	0.117
P06BX3	9.97	2.62	33.0	1.088	1.961	0.086	0.156
P06BX3	9.97	2.62	17.0	0.827	1.284	0.128	0.198
P07BY3	9.96	3.46	49.0	1.040	1.822	0.073	0.129
P07BY3	9.96	3.46	33.0	0.957	1.600	0.100	0.168
P07BY3	9.96	3.46	17.0	0.639	0.893	0.130	0.182
P08BZ3	9.90	5.25	49.0	0.899	1.452	0.096	0.156
P08BZ3	9.90	5.25	33.0	0.687	0.987	0.109	0.157
P08BZ3	9.90	5.25	17.0	0.447	0.563	0.138	0.174
P09CW3	15.15	2.15	49.0	1.422	3.134	0.062	0.137
P09CW3	15.15	2.15	33.0	1.500	3.467	0.098	0.226
P09CW3	15.15	2.15	17.0	1.073	1.922	0.136	0.243
P10CX3	15.15	2.62	49.0	1.359	2.881	0.073	0.154
P10CX3	15.15	2.62	33.0	1.348	2.840	0.107	0.226
P10CX3	15.15	2.62	17.0	0.931	1.534	0.144	0.237
P11CY3	15.12	3.46	49.0	1.190	2.278	0.084	0.161
P11CY3	15.12	3.46	33.0	1.154	2.165	0.121	0.227
P11CY3	15.12	3.46	17.0	0.789	1.199	0.161	0.244
P12CZ3	15.00	5.25	49.0	0.948	1.576	0.102	0.169
P12CZ3	15.00	5.25	33.0	0.866	1.373	0.138	0.218
P12CZ3	15.00	5.25	17.0	0.550	0.733	0.170	0.226

[a]NTU - number of transfer units.

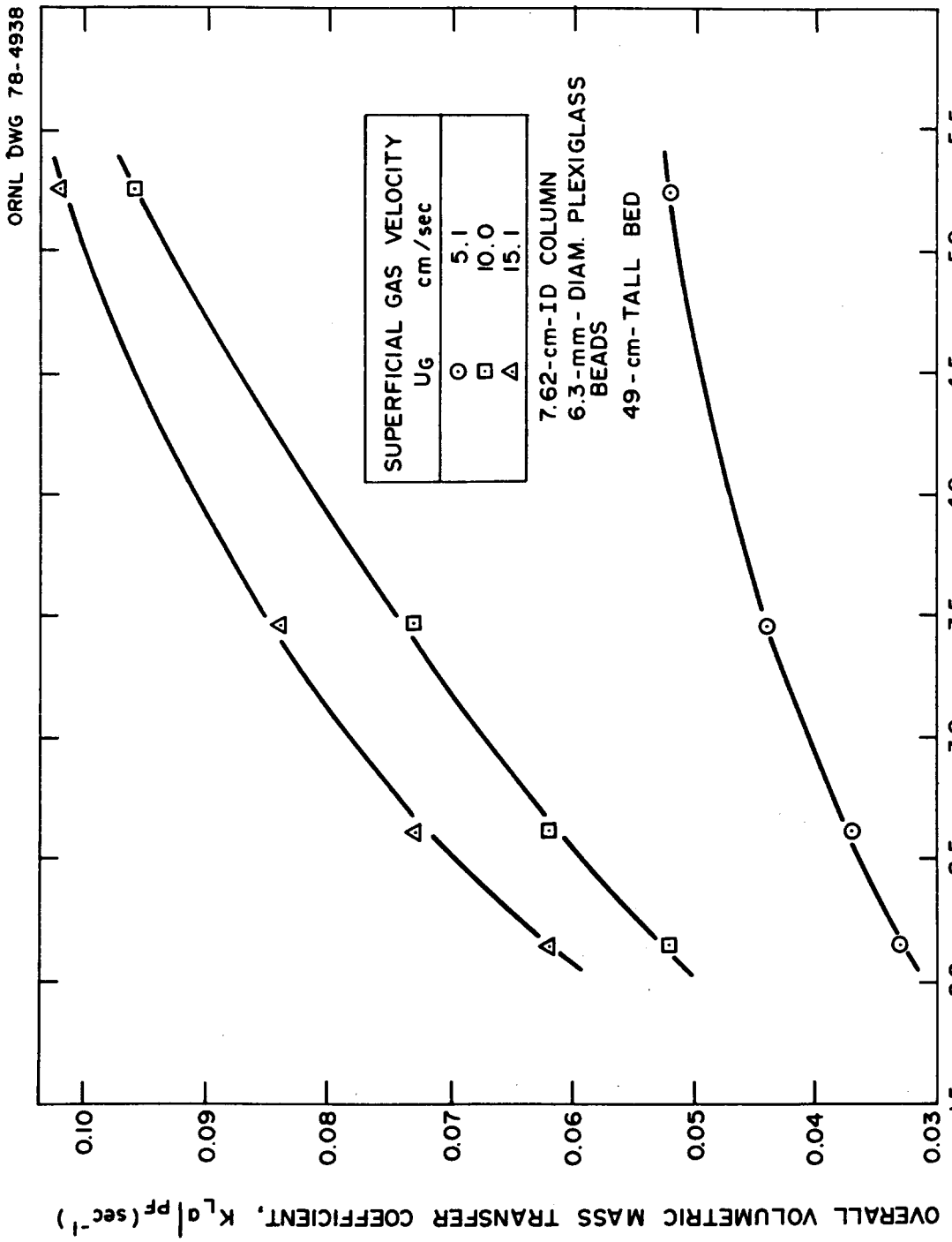

Fig. 2.28. Effect of gas velocity on the overall volumetric mass transfer coefficient in beds of 6.3-mm-diam plexiglass beads.

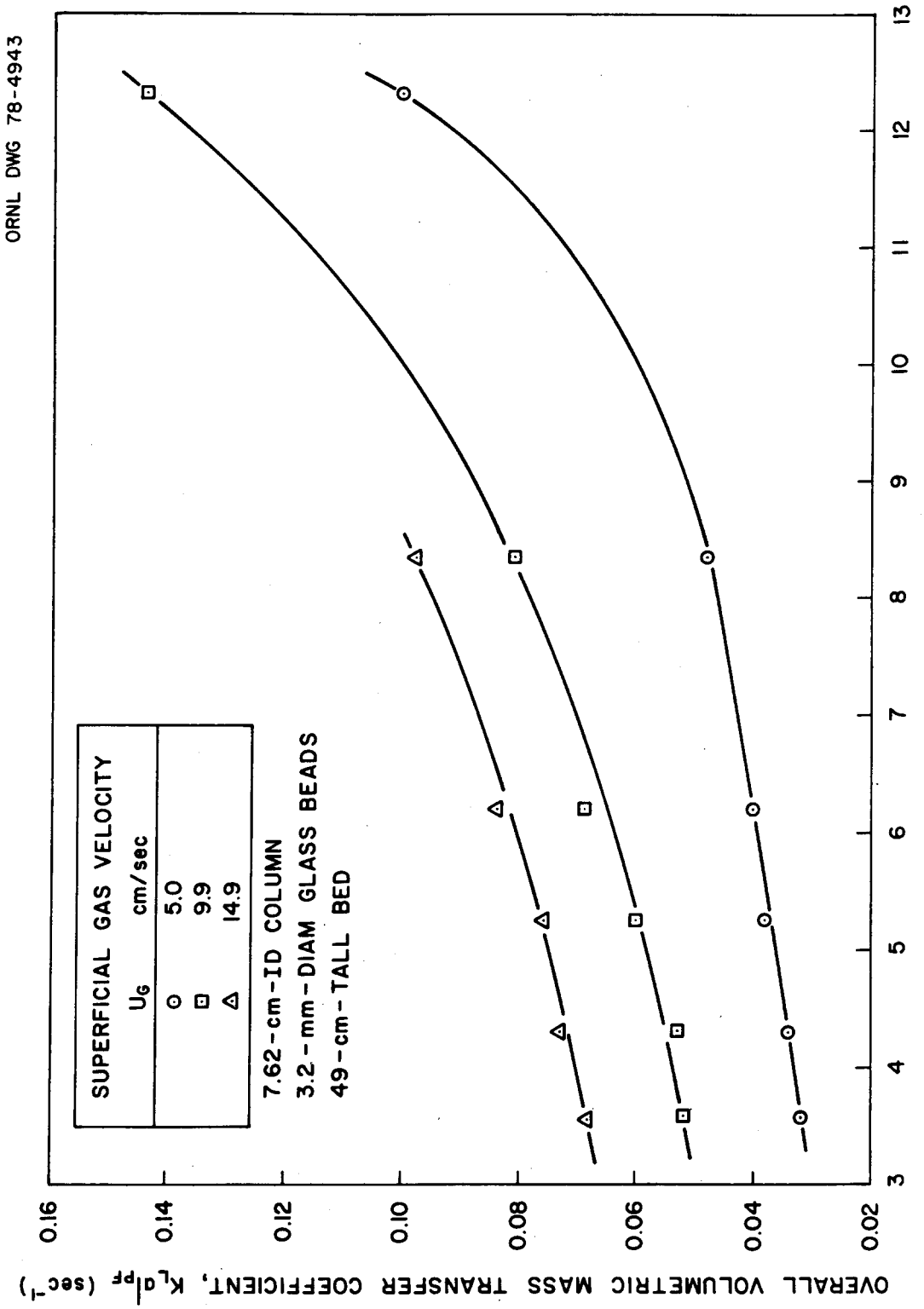

Fig. 2.29. Effect of gas velocity on $K_L a$ in beds of 3.2-mm-diam glass beads.

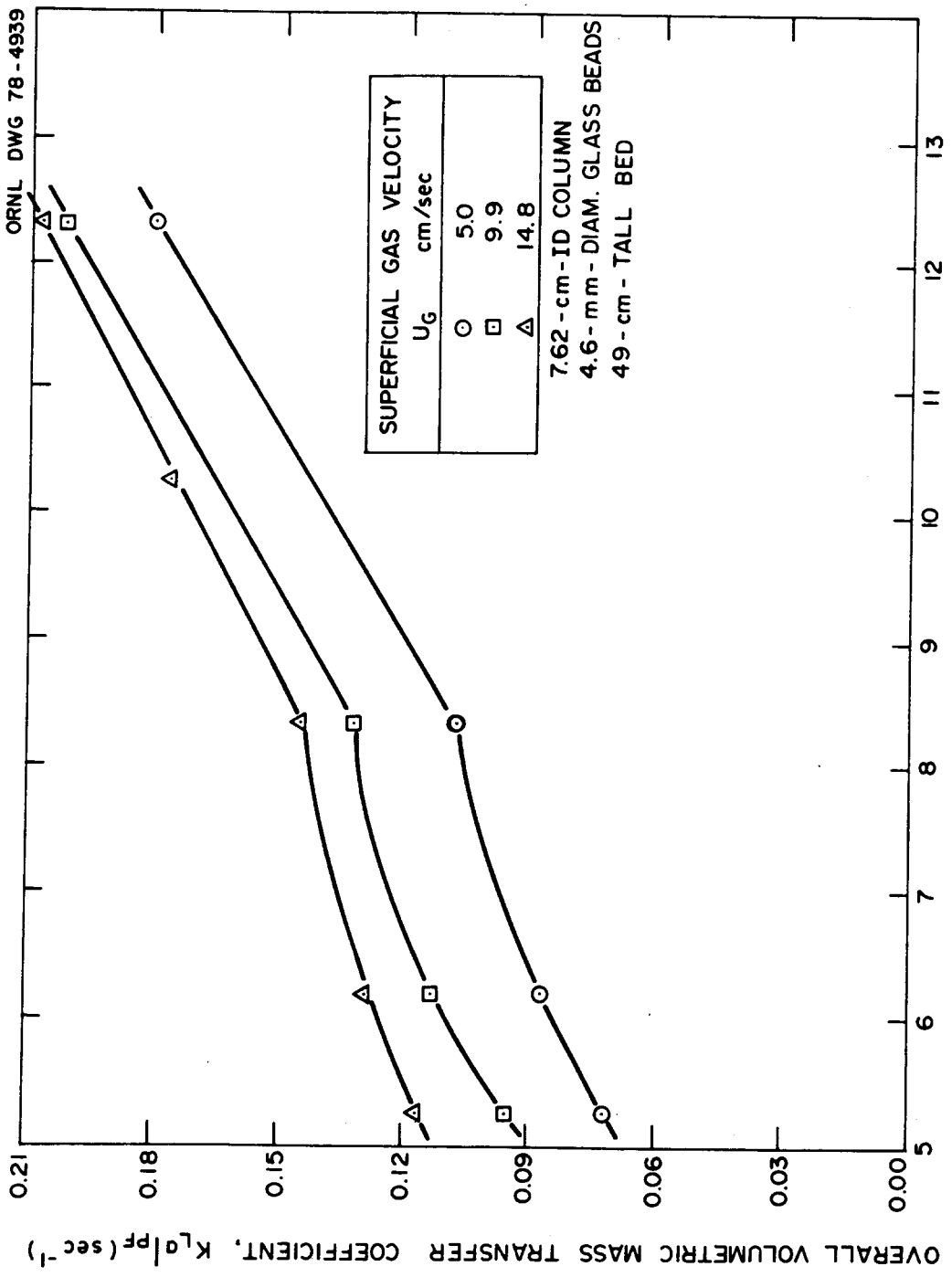

Fig. 2.30. Effect of gas velocity on K_La in beds of 4.6-mm-diam glass beads.

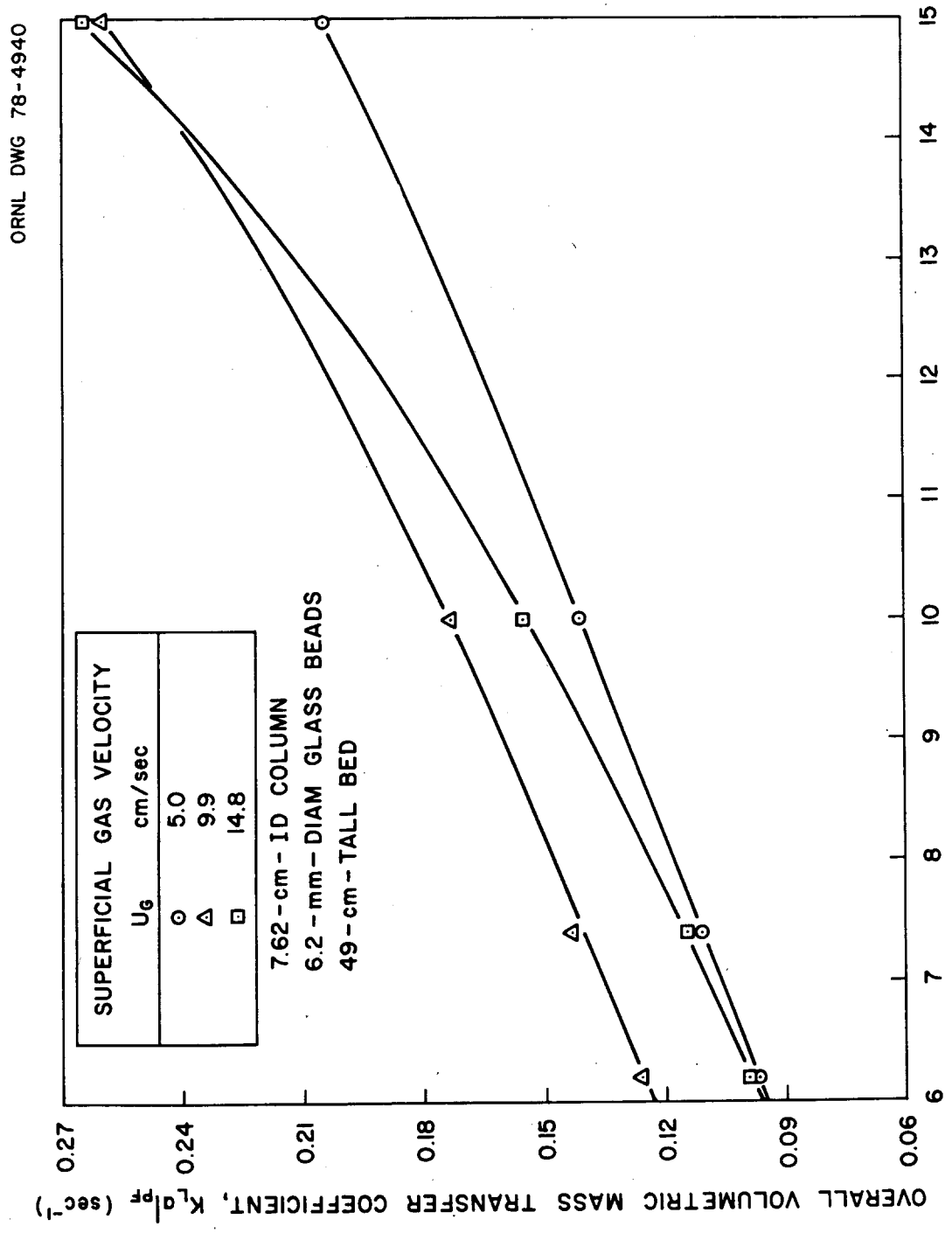

Fig. 2.31. Effect of gas velocity on K_La in beds of 6.2-mm-diam glass beads.

figures show, the relationship between $K_L a$ and the fluid velocities is apparently exactly the same in any of the systems. For example, Fig. 2.28 indicates a less than linear dependence of $K_L a$ on the liquid velocity, whereas Fig. 2.29 indicates a greater than linear dependence. In Fig. 2.28 the increase in $K_L a$ for an increase in the velocity from 5.1 to 10 cm/sec is much larger than that observed for a similar gas velocity change in the other systems. Figure 2.31 illustrates that the curves for gas velocities of 5.0 and 9.9 cm/sec are joined at a liquid velocity of 6 cm/sec, but as the liquid velocity is increased to 15 cm/sec, the curve for a gas velocity of 9.9 cm/sec diverges until it merges and actually crosses the curve for a gas velocity of 14.8 cm/sec.

Figure 2.32 shows the effect of particle size and density on $K_L a$, at a constant gas velocity of 5.0 cm/sec. The mass transfer coefficient increases with both increasing particle diameter and density. Apparently, the larger diameter of the plexiglass beads coupled with their much lower particle density results in mass transfer behavior similar to that exhibited by the 3.2-mm-diam glass beads. Figure 2.33 presents a similar example in which the gas velocity was kept constant at 9.9 cm/sec.

These results can be explained in terms of the type of bubble flow regime encountered in a three-phase fluidized bed. Large or heavy solids tend to break up the gas bubbles, giving rise to a "bubble-breakup" or "bubble-disintegration" regime. Small or light solids, however, do not break up the gas bubbles but allow them to coalesce; this is termed the "bubble-coalescence" regime. In the former regime, the bubbles are small (hence the surface area is very large), which increases the volumetric mass transfer coefficient. In the latter regime, the bubbles are large

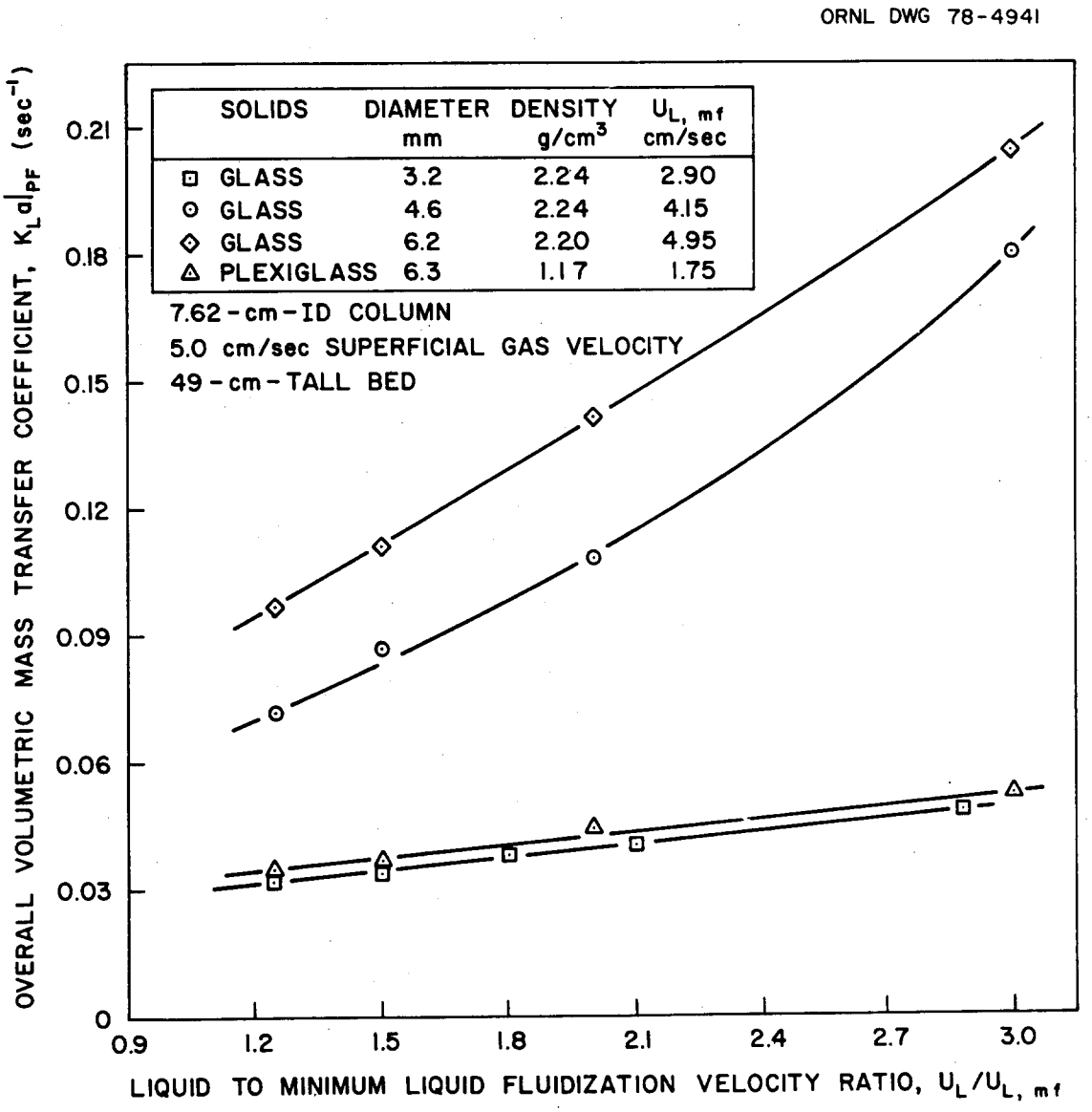

Fig. 2.32. Effect of particle size and density on $K_L a$ at a constant gas velocity of 5 cm/sec.

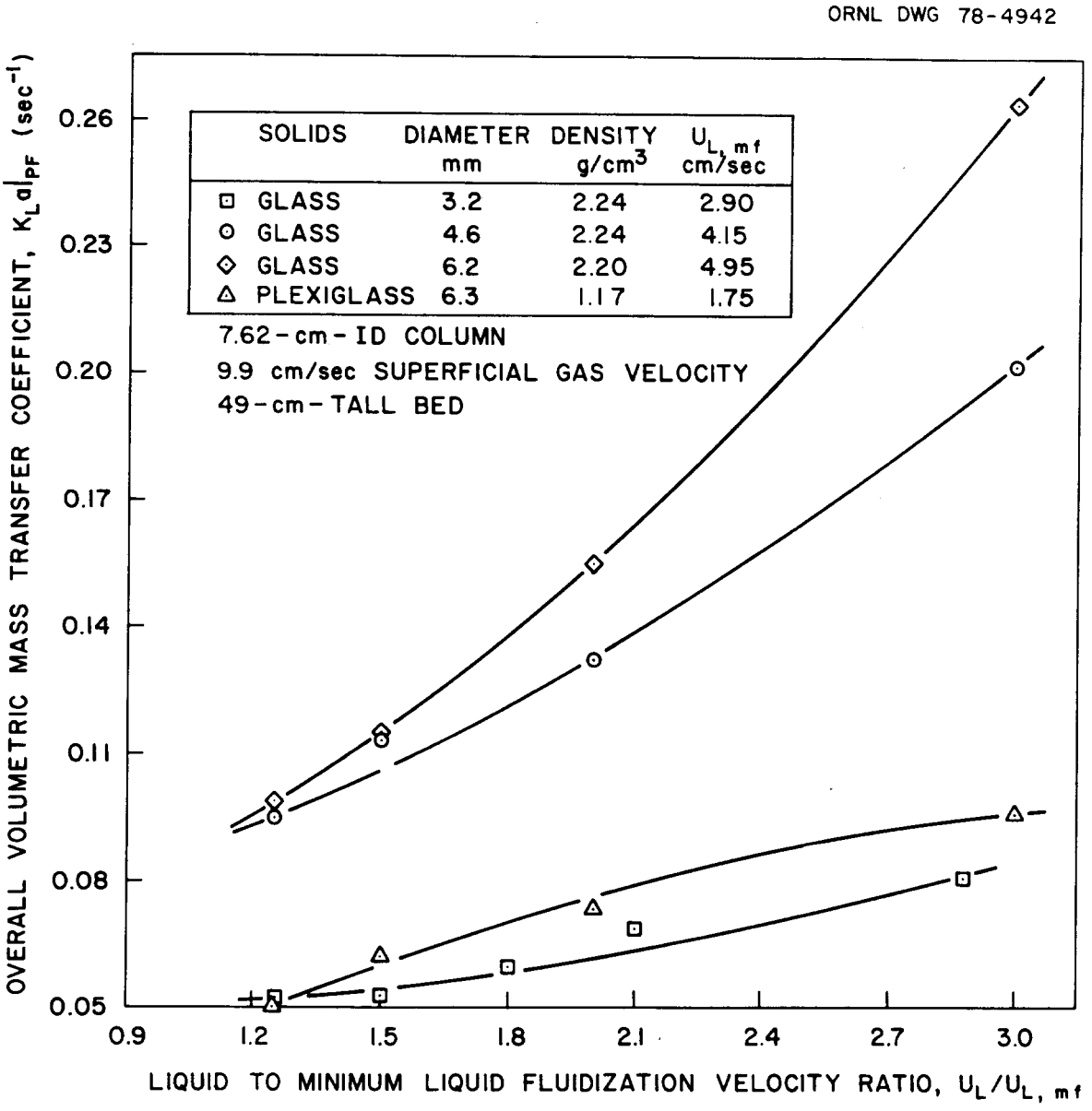

Fig. 2.33. Effect of particle size and density on $K_L a$ at a constant gas velocity of 9.9 cm/sec.

(hence the surface area is low) which decreases $K_L a$. Thus, use of the 3.2-mm-diam glass beads (small diameter) and the 6.3-mm-diam plexiglass beads (large diameter and low solid density) results in lower mass transfer coefficients than those obtained using the 4.6- and 6.2-mm-diam glass beads.

These mass transfer results were obtained by ignoring the effect of dispersion in the liquid phase as well as the column entrance and end effects. Future mass transfer experiments will attempt to deal with these phenomena. Experiments with the 15.2-cm-ID column are also planned. These will study the effect of column diameter and will use aqueous glycerol solutions to study the effect of liquid viscosity on the overall volumetric mass transfer coefficient.

2.5.3 Correlation of results

The results shown in the previous section and in previous reports[1,2,7] for MF velocities, overall phase holdups, and local phase holdups were correlated with the physical parameters of the systems studied by using multiple linear regression. Dimensional correlations were tried first and were followed by dimensionless correlations whenever possible. The predictive equations presented in this section represent the best of the many correlations that were attempted.

Minimum fluidization. The MF velocities shown in Fig. 2.23, along with the previously reported MF results in aqueous glycerol, were correlated with the system parameters and resulted in the following dimensionless correlation:

$$Re_{mf} = aAr^{b}Fr_{G}^{c} , \qquad (7)$$

where

Re_{mf} = Reynolds number = $\rho_L U_{L,mf} d_p / \mu_L$,

Ar = Archimedes number = $d_p^3 \rho_L (\rho_S - \rho_L) g / \mu_L^2$,

Fr_G = Froude number = $U_G^2 / g d_p$,

ρ_L = liquid density,

d_p = particle diameter,

μ_L = liquid viscosity,

ρ_S = solid density,

g = acceleration due to gravity,

U_G = gas velocity,

and the constants and their 95% confidence limits are

a = 0.005131 ± 0.002,

b = 0.661 ± 0.034,

c = -0.120 ± 0.025.

Equation (7) had a correlation coefficient of 0.94 and an F-value of 478 using a total of 135 points; it is shown in Figs. 2.34-2.36 as predicted versus experimental MF data. Although the overall correlation is very good, significant deviations can be seen between the predicted and experimental results under some conditions. Considering the range of conditions covered, though, the correlation is satisfactory. Several correlations were tested but Eq. (7) gave the best results. Note that Eq. (7) is not valid for a zero gas rate where it would predict a liquid MF velocity of zero. As Figures 2.34-2.36 show, however, if a predicted MF curve is generated starting with gas velocities just greater than zero, the MF curves can be reliably extrapolated back to zero gas flow. Alternatively, at zero gas velocity, the two-phase correlation of Wen and Yu[37] can be used to predict the MF velocity.

ORNL DWG 78-541R

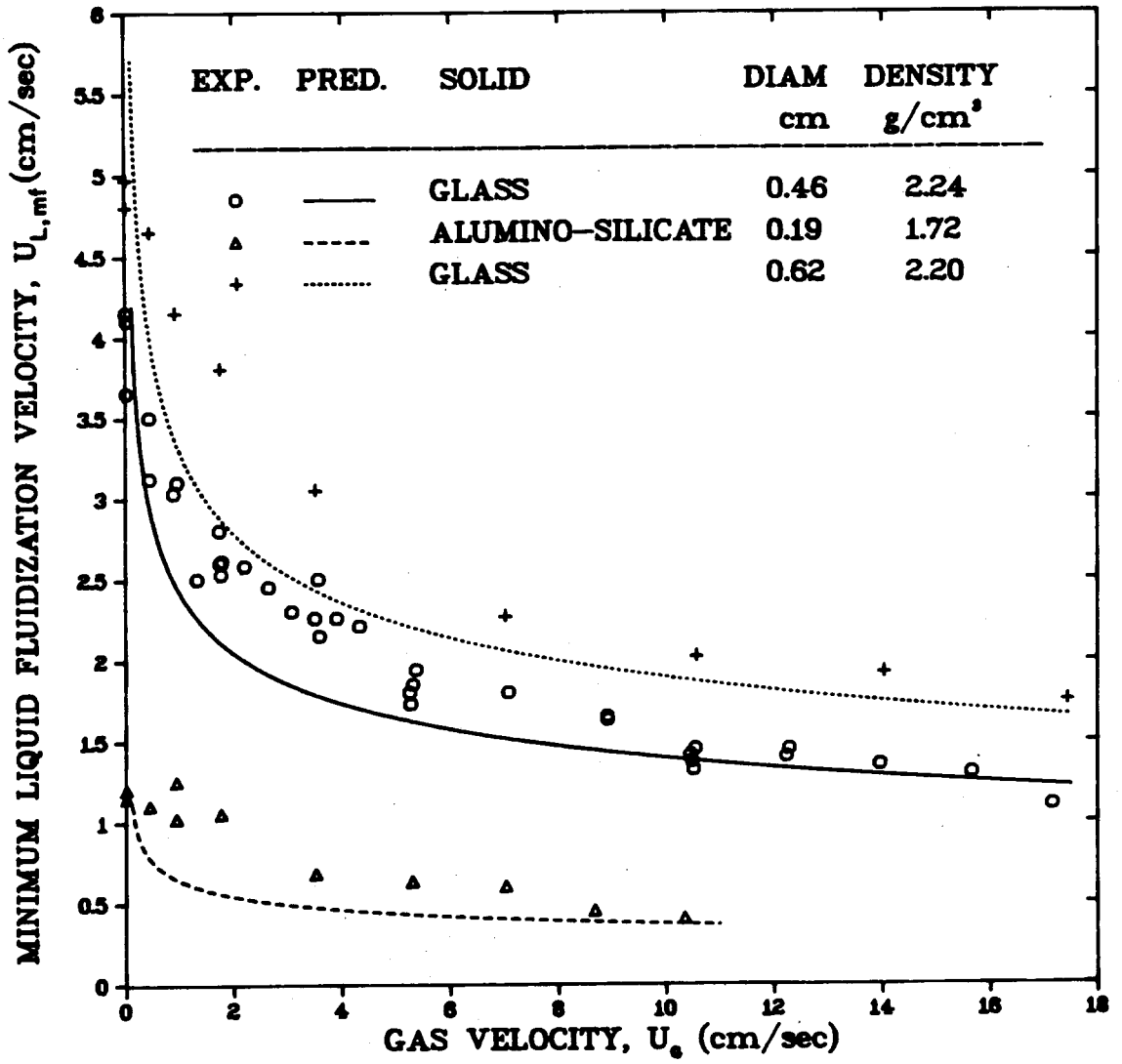

Fig. 2.34. Predicted vs experimental MF data for the glass and alumino-silicate beads.

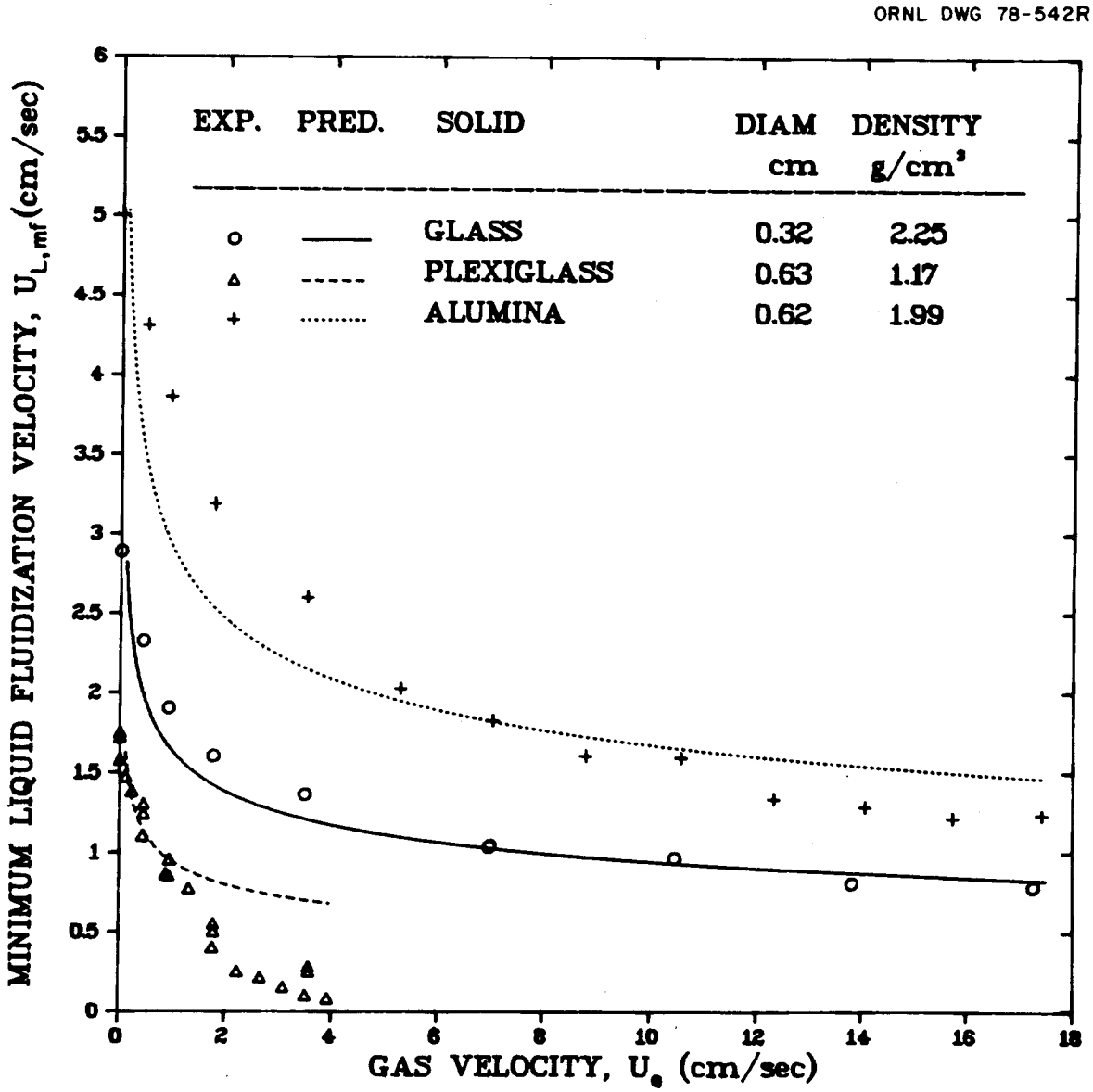

Fig. 2.35. Predicted vs experimental MF data for the glass, plexiglass, and alumina beads.